Journal of Zhejiang University-SCIENCE A (Applied Physics & Engineering)
ISSN 1673-565X (Print); ISSN 1862-1775 (Online)
www.zju.edu.cn/jzus; www.springerlink.com
E-mail: jzus@zju.edu.cn

Evaporate prediction and compensation of intake port wall-wetting fuel film for spark ignition engines fueled with ethanol-gasoline blends*

Dong-wei YAO†, Xin-chen LING, Feng WU†‡

(*Institute of Power Machinery and Vehicular Engineering, Zhejiang University, Hangzhou 310027, China*)

†E-mail: cyril1205@163.com; wfice@cmee.zju.edu.cn

Received Mar. 13, 2012; Revision accepted July 16, 2012; Crosschecked July 20, 2012

Abstract: The fuel dynamic transfer process, including fuel injection, fuel film deposition and evaporation in the intake port, was analyzed for spark ignition (SI) engines with port fuel injection (PFI). The influence of wall-wetting fuel film, especially its evaporation rate, upon the air-fuel ratio of in-cylinder mixtures was also discussed. According to the similarity principle, Fick's law, the ideal gas equation and the Gilliland correlation, an evaporate prediction model of wall-wetting fuel film was set up and an evaporate prediction based dynamic fuel film compensator was designed. Through engine cold start tests, the wall-wetting temperature, which is the key input of the fuel film evaporate prediction model, was also modeled and predicted. Combined with the experimental data of the evaporation characteristics of ethanol-gasoline blends and engine calibration tests, all the parameters of the wall-wetting fuel film evaporate prediction model used in the fuel film compensator were identified. Square-wave disturbance tests of fuel injection showed that with the help of the fuel film compensator the response of the in-cylinder air-fuel ratio was significantly improved and the real air-fuel ratio always closely matched the expected ratio. The fuel film compensator was then integrated into the final air-fuel ratio controller, and the engine tests showed that the air-fuel ratio control error was less than 2% in steady-state conditions, and less than 4% in transient conditions. The fuel film compensator also showed good adaptability to different ethanol-gasoline blends.

Key words: Spark ignition (SI) engine, Ethanol-gasoline blend, Wall-wetting effect, Evaporate prediction, Fuel film compensation
doi:10.1631/jzus.A1200068 **Document code:** A **CLC number:** TK417

1 Introduction

With the world's automobile production and population increasing year by year, the shortage of traditional fossil fuels and vehicle exhaust pollution have been growing problems. Various potential alternative fuels for vehicles have been proposed (Lave and Maclean, 2000). Among them, alcohol fuels have attracted widespread attention for their renewability and better performance in engine combustion and exhaust emissions (Celik, 2008; Najafi *et al*., 2009; Charoenphonphanich *et al*., 2011). As one of the most important alcohol fuels, ethanol-gasoline blends have been widely used in America, Brazil, New Zealand and some other countries (Pontoppidan *et al*., 2008; Anderson *et al*., 2012). In China, ethanol-gasoline blends also began to be used in 2000, and now have been promoted throughout the whole country.

Ethanol-gasoline blends have great potential to enhance the performance of conventional spark ignition (SI) engines. However, due to the extra added component of ethanol, the latent heat of vaporization, saturated vapor pressure, and molar vaporization enthalpy of the mixed fuels are changed (Balabin *et al*., 2007; Kar *et al*., 2008). This affects the evaporation characteristics of mixed fuels and the formation process of in-cylinder mixtures (Lauer *et al*., 2011).

‡ Corresponding author

* Project (Nos. 51106136 and 50776078) supported by the National Natural Science Foundation of China

For port fuel injection (PFI) engines, the injected fuel has a tendency to adsorb on the intake port wall because of the lower temperature there and form a wall-wetting fuel film. Most of the in-cylinder mixtures need to be generated by film evaporation. The wall-wetting fuel film mass and its evaporation rate directly affect the air-fuel ratio of in-cylinder mixtures, and even the performance of the whole engine (Kiencke and Nielsen, 2005). Fuel wall-wetting compensation for PFI SI engines has been widely studied (Arsie *et al*., 2003; Shan *et al*., 2008). However, most studies described the fuel film behavior of SI engines using an engineering approach rather than developing a theoretical solution of the wall-wetting phenomenon itself. For SI engines fueled with ethanol-gasoline blends, even no studies about the evaporation and compensation of wall-wetting fuel films have been seen yet.

In this paper, the fuel dynamic transfer process, including fuel injection, fuel film deposition and evaporation in the intake port of PFI SI engines was analyzed first. The influence of wall-wetting fuel film, especially its evaporation rate, upon the air-fuel ratio of in-cylinder mixtures was then discussed. Both the intake air flow and the intake port wall temperature are crucial factors for fuel film evaporation. By regarding the wall-wetting fuel film evaporation in the intake port as a tube forced convective mass transfer process, combined with Fick's law, the ideal gas equation and the Gilliland correlation, an evaporate rate prediction model of wall-wetting fuel film was set up, then improved and verified with engine experimental data. On this basis, an evaporate prediction based dynamic fuel film compensator for SI engines fueled with ethanol-gasoline blends was designed. All bench tests were carried out on a MR479Q model PFI SI engine, and the results showed that the compensator works efficiently and reliably. It has good adaptability to different ethanol-gasoline blends and can be directly applied to air-fuel ratio control strategy design, especially for PFI SI engines fueled with ethanol-gasoline blends.

2 Port fuel injection and wall-wetting effect

Due to the lower temperature in the intake port of PFI SI engines, the injected fuel has a tendency to adsorb on the intake port wall and form a wall-wetting fuel film. The film evaporates after being heated, and flows in vapor form into cylinders to participate in combustion. The whole fuel dynamic transfer process during port fuel injection can be seen in Fig. 1.

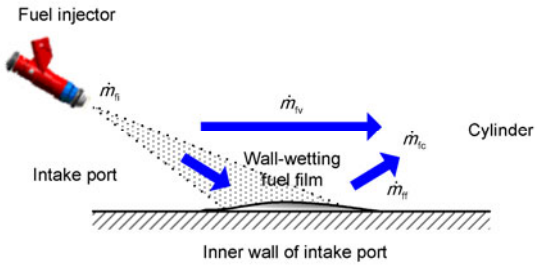

Fig. 1 Schematic diagram of port fuel injection

In Fig. 1, $\dot{m}_{fi}$ and $\dot{m}_{fc}$ are the fuel mass flows from injectors and into cylinders, $\dot{m}_{fv}$ is the unabsorbing fuel vapor mass flow, and $\dot{m}_{ff}$ is the evaporated fuel mass flow from the wall-wetting fuel film. The dynamic transfer process of intake port wall-wetting fuel film can be described as (Aquino, 1981)

$$\begin{cases} \dot{m}_{f} = X\dot{m}_{fi} - \dfrac{m_{f}}{\tau}, \\ \dot{m}_{fc} = \dot{m}_{fv} + \dot{m}_{ff} = (1-X)\dot{m}_{fi} + \dfrac{m_{f}}{\tau}, \end{cases} \tag{1}$$

where τ is the fuel film evaporation time, X is the fuel adsorption ratio, and m_f is the fuel film mass. By Laplace transform, the transfer function of fuel film dynamic transfer process, Eq. (1) can be derived as

$$G_{f}(s) = \frac{\dot{m}_{fc}(s)}{\dot{m}_{fi}(s)} = \frac{1+(1-X)\tau s}{1+\tau s}. \tag{2}$$

Therefore, the unit step response of in-cylinder fuel mass flow can be obtained by inverse Laplace transform as

$$\dot{m}_{fc}(t) = L^{-1}\left(G_{f}(s)\cdot\frac{1}{s} \right) = 1 - X\cdot \mathrm{e}^{-t/\tau}. \tag{3}$$

Due to the existence of the fuel wall-wetting effect, the actual in-cylinder fuel mass flow cannot closely match the injected fuel mass flow from the

injectors. After a sudden rise of $1-X$ proportion, it will gradually approach the expected fuel mass flow from injectors along an exponential curve. The approach rate greatly depends on the fuel film evaporation time τ (Fig. 2).

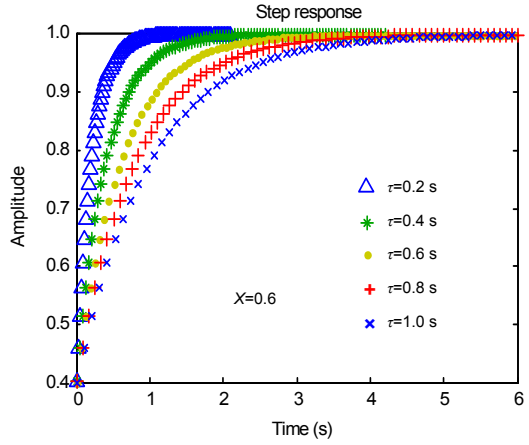

Fig. 2 Step response of fuel dynamic transfer process

The wall-wetting effect in the intake port causes hysteresis errors in the in-cylinder fuel mass flow, which lead to deviations in the air-fuel ratio from the expected values. The slower the fuel film evaporates, the larger and longer are the deviations. The evaporation of fuel film is affected by a variety of factors, such as its chemical composition (e.g., ethanol content), intake air flow, and intake port wall temperature where fuel injection occurs. To reduce the negative impact of the wall-wetting effect on air-fuel ratio control, the fuel film evaporation rate must be accurately predicted and compensated before delivering the desired amount of fuel to the fuel injectors.

3 Fuel film evaporation rate modeling

The net molar diffusion flux of evaporated fuel from a wall-wetting fuel film to the intake air stream N_f can be derived according to Fick's law as

$$N_f = h_m(c_{f,w} - c_{f,\infty}) = \frac{m_f}{\tau M_f A_f}, \tag{4}$$

where h_m is the mass transfer coefficient, M_f is the average molecular weight of the mixed fuel, A_f is the surface area of fuel film exposed to the intake air stream, and $c_{f,w}$ and $c_{f,\infty}$ are the fuel vapor concentrations near the fuel film surface and in the intake air stream, respectively. As $c_{f,w} >> c_{f,\infty}$, $c_{f,\infty}$ can be neglected. $c_{f,w}$ can be derived according to the ideal gas equation as

$$c_{f,w} = \frac{p_s}{RT_f}, \tag{5}$$

where p_s is the fuel saturated vapor pressure, T_f is the fuel film temperature, and R is the molar gas constant. For ethanol-gasoline blends, the fuel saturated vapor pressure can be predicted by the Clausius-Clapeyron equation as

$$p_s = p_{s0} e^{-\frac{\Delta H}{RT_f}}, \tag{6}$$

where p_{s0} is the fuel saturated vapor pressure constant, and ΔH is the fuel molar gasification enthalpy. According to Eqs. (4)–(6), the fuel film evaporation time can be derived as

$$\frac{1}{\tau} = \frac{1}{m_f} M_f A_f h_m \frac{p_{s0}}{RT_f} e^{-\frac{\Delta H}{RT_f}}. \tag{7}$$

If the wall-wetting fuel film evaporation in the intake port is treated as a tube forced convective mass transfer process, then the mass transfer coefficient h_m can be derived by the Gilliland correlation as

$$h_m \propto \frac{D_f}{d} Re^{0.83} Sc^{0.44} \propto \frac{D_f}{d} \dot{m}_a^{0.83} \left(\frac{T_i}{p_i}\right)^{0.44}, \tag{8}$$

where D_f is the fuel diffusion coefficient, and d is the inner diameter of intake port. Re and Sc are the Reynolds number and Schmidt number, both of which can be replaced by several engine condition parameters (Maloney, 1999), such as the intake air mass flow $\dot{m}_a$, the intake air pressure p_i, and the intake air temperature T_i. From Eqs. (7) and (8), the final fuel film evaporation time model can be derived as

$$\frac{1}{\tau} \propto \left(\frac{A_f}{m_f}\right) \cdot \left(\frac{D_f M_f p_{s0}}{Rd}\right) \cdot \dot{m}_a^{0.83} \left(\frac{T_i}{p_i}\right)^{0.44} T_f^{-1} e^{-\frac{\Delta H}{RT_f}}. \tag{9}$$

The first item on the right side of Eq. (9) is the specific surface area of the fuel film, while the second item and ΔH all depend on the properties of ethanol-gasoline blends. By introducing a fuel-related calibration parameter C_f, Eq. (9) can be simplified as

$$\frac{1}{\tau}=C_f\cdot\dot{m}_a^{0.83}\left(\frac{T_i}{p_i}\right)^{0.44}T_f^{-1}e^{-\frac{\Delta H}{RT_f}}. \tag{10}$$

In Eq. (10), there is almost no feasible means to measure the wall-wetting fuel film temperature in the intake port of a real engine. However, in view of the small mass and thermal inertia of the wall-wetting fuel film, its temperature can be evaluated by the nearby intake wall temperature. Many studies have been made on the heat transfer near the wall-wetting fuel film and the intake valves (Cowart and Cheng, 1999; Maloney, 1999; Alkidas, 2001). According to previous studies, the wall-wetting temperature can be considered to follow a first-order inertial system as

$$f_t\dot{T}_f+T_f=f_s, \tag{11}$$

where f_t is the transient time constant and f_s is the steady state item. Both are associated with a variety of engine condition parameters, and need to be calibrated. Thus, Eqs. (10) and (11) comprise the whole evaporation rate model of wall-wetting fuel film for PFI SI engines fueled with ethanol-gasoline blends.

4 Fuel-adaptive wall-wetting compensator design

The wall-wetting compensator should be designed to make sure that $\dot{m}_{fc}=\dot{m}_{fd}$, where $\dot{m}_{fd}$ is the desired in-cylinder fuel mass flow. Thus, according to Eq. (1), the dynamic transfer process model of an intake port wall-wetting fuel film, the injected fuel mass flow $\dot{m}_{fi}$ should be compensated as

$$\begin{cases}\dot{m}_{fi}=\dfrac{1}{1-X}\left(\dot{m}_{fd}-\dfrac{m_f}{\tau}\right),\\ \dot{m}_f=X\dot{m}_{fi}-\dfrac{m_f}{\tau}.\end{cases} \tag{12}$$

For 4-cylinder 4-stroke SI engines, the update cycle of $\dot{m}_{fi}$ can be synchronized with the engine speed n. Thus, the update period of the compensator is consistent with the engine duty cycle, as

$$t_c=120/n. \tag{13}$$

According to the updating period, the discrete form of the compensator Eq. (12) can be derived as

$$\begin{cases}m_{fi,i}(k)=\dfrac{m_{fd,i}(k)-(1-\alpha)m_{fi}(k-1)}{1-X},\\ m_{fi}(k)=Xm_{fi,i}(k)+\alpha m_{fi}(k-1),\end{cases} \tag{14}$$

where the subscript i is the cylinder number, $\alpha=e^{-120/(n\tau)}$. From Eq. (14), the best fuel mass to be injected after compensation depends not only on the desired in-cylinder fuel mass, but also on the evaporated fuel mass from the previous wall-wetting fuel film. Here, α can be seen as a residual coefficient of fuel film evaporation during the previous engine cycle. The current fuel film mass is the sum of the residual fuel film in the previous cycle and the newly adsorbing fuel in the current cycle (Fig. 3).

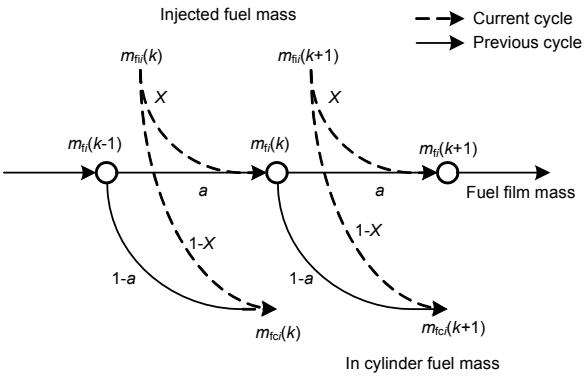

Fig. 3 Mass balance diagram of the wall-wetting fuel film

Through Laplace transform, the transfer function of the discrete fuel film compensator Eq. (14) can be derived as

$$G_c(z)=\frac{m_{fi,i}(z)}{m_{fd,i}(z)}=\frac{z-\alpha}{(1-X)z+X-\alpha}. \tag{15}$$

To ensure adequate stability, the only pole of the compensator must be put on the positive real axis and

within the unit circle on the complex plane.

$$0 \le \frac{\alpha - X}{1 - X} < 1 \Rightarrow 0 < X < \alpha. \tag{16}$$

The final block diagram of the fuel film compensator used for PFI SI engines is shown in Fig. 4. The residual coefficient α reflects the evaporation rate of the wall-wetting fuel film, and can be calculated using Eqs. (10) and (11). The fuel adsorption ratio X is affected by many factors, especially the structure and location of injectors and the intake air flow. In practical application, X can be determined by engine calibration tests with the restriction only of Eq. (16). Both α and X can be optimized automatically according to the current blend ratio γ of ethanol-gasoline blends. Thus, the compensator is adaptive to different mixed fuels. T_w is the cooling water temperature.

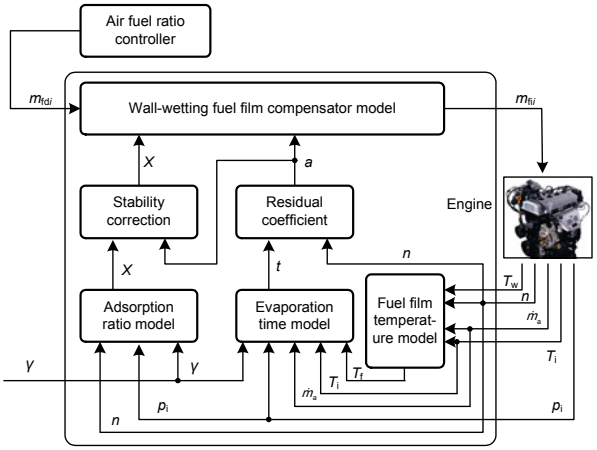

Fig. 4 Block diagram of the fuel-adaptive wall-wetting fuel film compensator

5 Model improvement and parameter identification

5.1 Wall-wetting temperature model improvement

A 4-cylinder, 4-stroke, 1.342 L, MR479Q model PFI SI engine equipped with a self-developed engine management system (EMS) (Yao, 2010) was chosen for the bench tests. A copper-constantan thermocouple was installed near the intake valve of the second cylinder to detect the wall-wetting temperature for model identification of Eq. (11) (Fig. 5).

Fig. 6 shows the temperature histories during engine warm-up under pure gasoline E0 (where the letter E represents the ethanol component, while the number indicates the ethanol volume percentage in the mixed fuel), with different engine speeds and intake air mass flows.

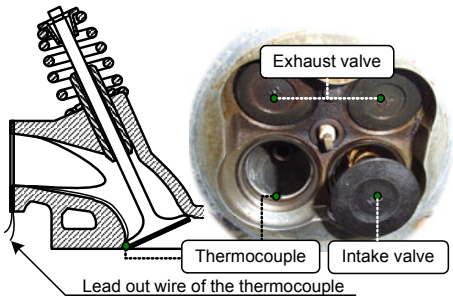

Fig. 5 Installation diagram of the thermocouple used for wall-wetting temperature detecting

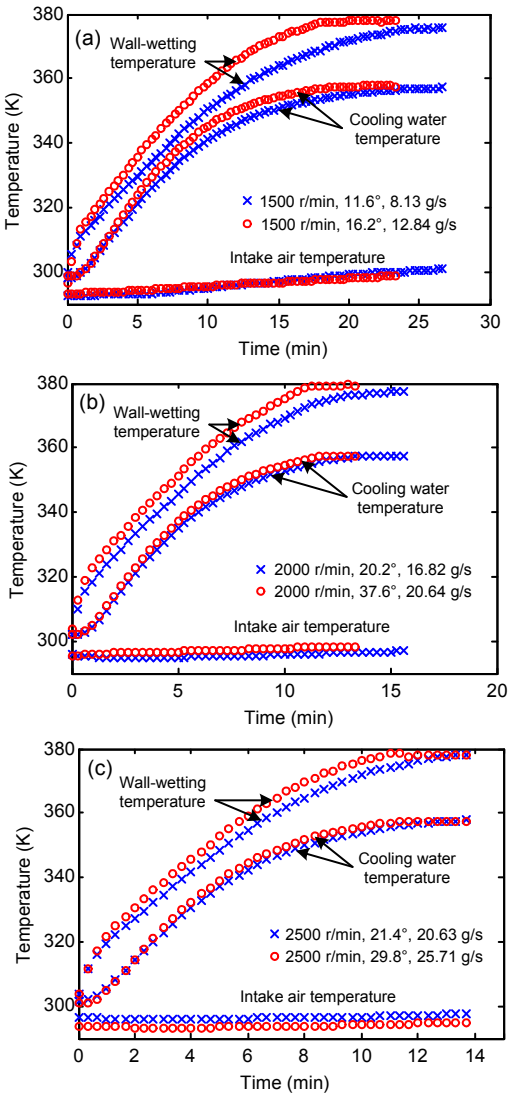

Fig. 6 Temperature histories during engine warm-up under 1500 r/min (a), 2000 r/min (b), and 2500 r/min (c)

From Eq. (11), the wall-wetting temperature should have the features of a first-order inertial system. However, from Fig. 6, the wall-wetting temperature history during engine warm-up can be divided into two stages: the rapid warm-up stage and the quasi-steady-state stage. The rapid warm-up stage lasts for 1−2 min, in which the wall-wetting temperature rises quickly and basically follows exponential functions as Eq. (11) describes. The intake air flow, which is related to the engine power, can accelerate the wall-wetting temperature rise. During the quasi-steady-state stage, the wall-wetting temperature no longer rises exponentially, but closely matches the cooling water temperature. Under the same engine speeds, the greater is the intake air flow, the higher becomes the quasi-steady value of the wall-wetting temperature, due to the increment of heat transfer flux from the combustion chamber to the intake port.

Fig. 7 shows the temperature histories during engine warm-up under the same intake air flow but different engine speeds. Because the intake air flow is the same, the wall-wetting temperature in the rapid warm-up stage is almost the same. But in the quasi-steady-state stage, the lower is the engine speed, the faster is the rise of the wall-wetting temperature, while the cooling water temperature shows almost no change. This is because the heat transfer flux from the combustion chamber to the intake port stays the same under the same intake air flow, and a higher engine speed would increase the power of the cooling system. Thus, the wall-wetting temperature would then decrease with the enhanced cooling effect.

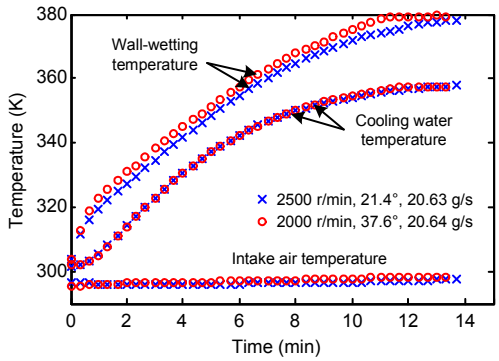

Fig. 7 Temperature histories during engine warm-up under the same intake air flow but different engine speeds

Based on this analysis, the wall-wetting temperature history during engine warm-up much depends on the heat transfer flux from the combustion chamber to the intake port (closely related to the intake air flow), especially in the rapid warm-up stage. In the quasi-steady-state stage, the quasi-steady value of the wall-wetting temperature is determined by the balance of several heat sources, such as the combustion chamber, the engine cooling system and the intake air flow. Therefore, the transient time constant and steady state item in Eq. (11) should be expressed as functions of several engine condition parameters as

$$f_t(\dot{m}_a)\dot{T}_f + T_f = f_s(\dot{m}_a, n, T_i, T_w). \tag{17}$$

The MATLAB parameter identification toolbox, introduced to identify the parameters of the wall-wetting temperature model Eq. (17), gave the result

$$\begin{cases} f_t = 39.3 + 0.74\dot{m}_a, \\ f_s = 0.82\dot{m}_a - 0.01n + 1.11T_i + 0.94T_w - 292.79. \end{cases} \tag{18}$$

Fig. 8 compares the results from the model calculation with the experimental data of wall-wetting temperatures. Clearly, the final wall-wetting temperature model Eq. (18) has high accuracy, with the maximum prediction error being less than ±6 K.

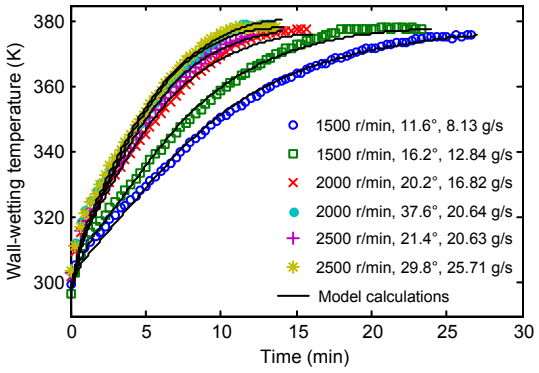

Fig. 8 Comparison of results from the model calculation and experimental data of wall-wetting temperatures

To investigate the influence of the ethanol component on the wall-wetting temperature, engine tests under different ethanol-gasoline blends were also carried out. Fig. 9 shows the temperature histories during engine warm-up under E0, E10, E20 and E30, with the same engine speed of 2000 r/min, and a throttle opening around of 19.7°.

For different ethanol-gasoline blends (including pure gasoline E0), the heat values of equivalent mixtures are roughly equal. Thus, under the same

engine operating conditions, the heat release rates of in-cylinder combustion with different mixed fuels are almost the same, leading to the high consistency of different cooling water temperature history curves in Fig. 9. However, due to the small mass and thermal inertia of the wall-wetting fuel film, the temperature difference caused by the properties of the mixed fuel itself is very small (Fig. 9). Therefore, besides E0, the wall-wetting temperature model of Eqs. (17) and (18) is also suitable for other ethanol-gasoline blends.

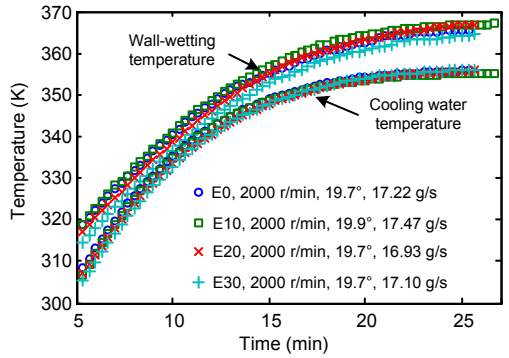

Fig. 9 Temperature histories during engine warm-up under different ethanol-gasoline blends

5.2 Fuel film evaporation rate model identification

The wall-wetting fuel film evaporation rate model of Eq. (10) still has two unknown parameters, C_f and ΔH, both of which are closely related to the properties of ethanol-gasoline blends. To identify them, the saturated vapor pressures of each ethanol-gasoline blend under different temperatures were tested (Fig. 10). From the results, it is obvious that the saturated vapor pressure of the mixed fuel has a strong exponential relationship with its temperature, as described in the Clausius-Clapeyron Eq. (6). Taking the logarithm of Eq. (6) derives

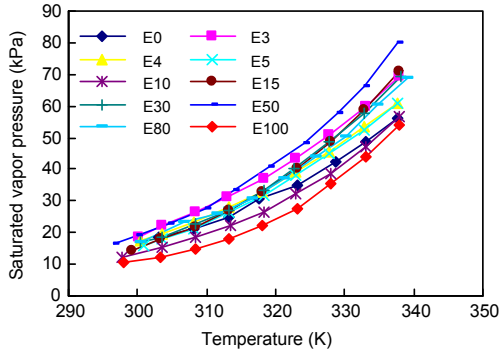

Fig. 10 Saturated vapor pressures of different ethanol-gasoline blends

$$\ln p_s = -\frac{\Delta H}{RT_f} + \ln p_{s0}. \tag{19}$$

Thus, the fuel molar gasification enthalpy ΔH can be obtained through linear regression of experimental data of $\ln p_s$ and T_f^{-1}. For C_f, the original fuel film dynamic parameters such as τ and X should first be calibrated based on the engine tests (Hendricks *et al.*, 1992). C_f can be then identified through linear regression according to Eq. (10). The identification results of the wall-wetting fuel film evaporation rate model under different ethanol-gasoline blends are summarized in Table 1.

Table 1 Parameter identification results of the wall-wetting fuel film evaporation rate model

Fuel type	C_f	ΔH (kJ/mol)
E0	1.122	27.87
E10	1.284	31.85
E20	1.216	33.46
E30	1.069	32.36

6 Bench test verification

The fuel-adaptive wall-wetting fuel film compensator of Fig. 4 was embedded into the self-developed EMS controller. All the engine verification tests were carried out on a MR479Q model PFI SI engine, and covered two kinds of bench tests, i.e., steady-state tests and transient-state tests.

6.1 Steady-state tests

During steady-state tests, the engine speed, throttle opening and intake air mass flow were all maintained at constant values. Thus, the in-cylinder air-fuel ratio would be influenced only by the intake port wall-wetting effect. A square-wave perturbation was adopted to be added on the desired fuel mass flow. The perturbation amplitude was maintained at around 8% of the stoichiometric fuel. The air-fuel ratio in-cylinder was detected in real time by an ETAS LA4 lambda meter which was mounted on the exhaust manifold.

Fig. 11 compares the results of the in-cylinder air-fuel ratio step response with and without the wall-wetting fuel film compensation. The mixed fuels E0 and E30, and engine speeds of 1500 r/min and 2000 r/min were adopted in the tests. In each figure,

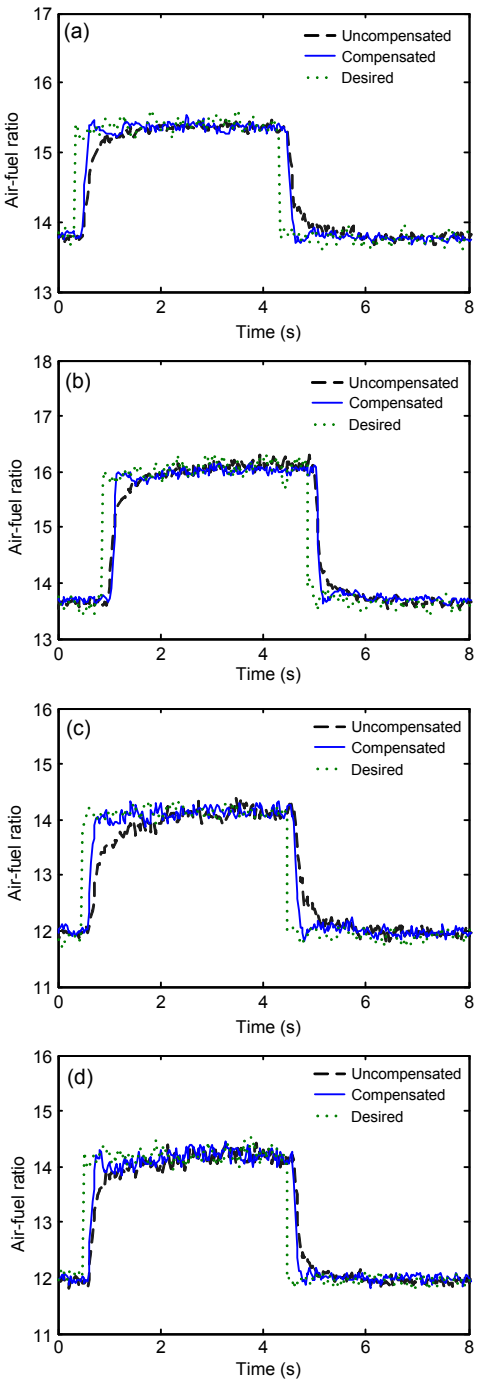

Fig. 11 Air-fuel ratio step response under E0, 1500 r/min, 20.7° (a), E0, 2000 r/min, 24.2° (b), E30, 1500 r/min, 20.7° (c), and E30, 2000 r/min, 24.2° (d)

the dotted line represents the desired in-cylinder air-fuel ratio under the fuel square-wave perturbation, the solid line and the dashed line represent the measured in-cylinder air-fuel ratio with and without the fuel film compensator, respectively.

The linear oxygen sensor of the ETAS LA4 lambda meter was mounted on the exhaust manifold where time would be needed for the air-fuel ratio to transmit from in-cylinder to the exhaust pipe. Thus, there was a time interval between the measured air-fuel ratios and the desired values. From Fig. 11, without fuel film compensation, a large deviation and time lag can be seen between the measured air-fuel ratios and the desired values due to the intake wall-wetting effect, especially at the beginning of the fuel step. In contrast, with the fuel film compensator, the air-fuel ratio response was significantly improved, and closer to the ideal square wave of the desired air-fuel ratio. The fuel-adaptive compensator was also effective for different ethanol-gasoline blends.

6.2 Transient-state tests

Further verification tests of the fuel film compensator during engine transient-state were carried out. Figs. 12 and 13 show the air-fuel ratio control results with fuel film compensation under E0 and E30, when a step disturbance of throttle opening exists.

Clearly, under both steady-state and transient-state conditions, the measured air-fuel ratios were all close to the corresponding stoichiometric ratios (for E10, 14.67; for E30, 12.87). The maximum relative deviation of the air-fuel ratio control during steady-state conditions did not exceed 2%. Under transient-state conditions, the deviation was slightly larger, but still within 4%. Generally speaking, the fuel film evaporation rate model accurately described the dynamic characteristics of the intake wall-wetting effect. The fuel film evaporate prediction based compensator had a good effect on the wall-wetting compensation of the air-fuel ratio control, and excellent adaptability to different ethanol-gasoline blends.

7 Conclusions

The intake wall-wetting effect of PFI SI engines causes hysteresis errors of in-cylinder fuel mass flow, leading to air-fuel ratio deviations from expected values. The slower the fuel film evaporates, the larger and longer are the deviations. Moreover, for PFI SI engines fueled with ethanol-gasoline blends, the extra component of ethanol has changed the evaporation characteristics of mixed fuels, making the already

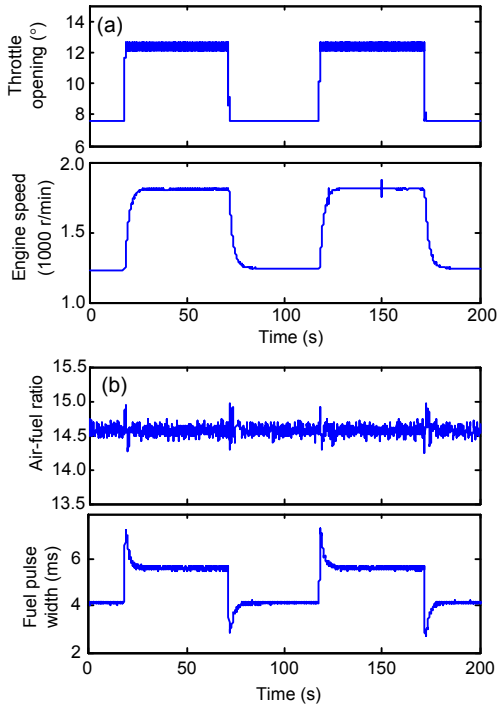

Fig. 12 Air-fuel ratio control effect under E0 with throttle opening and engine speed (a) and air-fuel ratio and fuel pulse width (b)

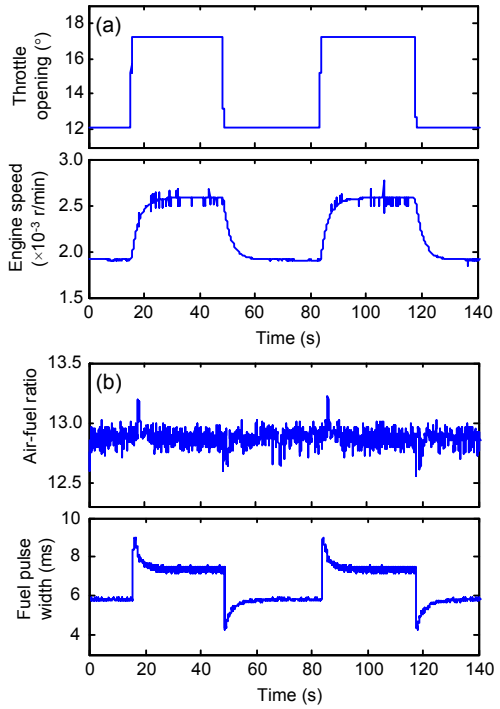

Fig. 13 Air-fuel ratio control effect under E30 with throttle opening and engine speed (a) and air-fuel ratio and fuel pulse width (b)

difficult intake wall-wetting fuel film compensation even more complex.

To reduce the impact of the wall-wetting effect on air-fuel ratio control and consider the influence of mixed fuels meanwhile, an evaporate prediction model of the wall-wetting fuel film with different ethanol-gasoline blends was set up according to Fick's law, the ideal gas equation and the Gilliland correlation. And then an evaporate prediction based fuel-adaptive dynamic wall-wetting compensator for PFI SI engines fueled with ethanol-gasoline blends was designed.

Square-wave disturbance tests of fuel injection showed that with the help of a fuel film compensator the response of the in-cylinder air-fuel ratio is significantly improved and the real air-fuel ratio always closely matches the expected ratio. Further verification results of air-fuel ratio control with the fuel film compensator showed that the air-fuel ratio control error is less than 2% under steady-state conditions, and less than 4% under transient conditions. In addition, the fuel film compensator has good adaptability to different ethanol-gasoline blends.

References

Alkidas, A., 2001. Intake-Valve Temperature Histories during SI Engine Warm-up. SAE Technical Paper, 2001-01-1704. [doi:10.4271/2001-01-1704]

Anderson, J.E., Dicicco, D.M., Ginder, J.M., Kramer, U., Leone, T.G., Raney-Pablo, H.E., Wallington, T.J., 2012. High octane number ethanol-gasoline blends: quantifying the potential benefits in the United States. *Fuel*, **97**: 585-594. [doi:10.1016/j.fuel.2012.03.017]

Aquino, C., 1981. Transient A/F Control Characteristics of the 5 Liter Central Fuel Injection Engine. SAE Technical Paper, 810494. [doi:10.4271/810494]

Arsie, I., Pianese, C., Rizzo, G., Cioffi, V., 2003. An adaptive estimator of fuel film dynamics in the intake port of a spark ignition engine. *Control Engineering Practice*, **11**(3):303-309. [doi:10.1016/S0967-0661(02)00040-0]

Balabin, R.M., Syunyaev, R.Z., Karpov, S.A., 2007. Molar enthalpy of vaporization of ethanol-gasoline mixtures and their colloid state. *Fuel*, **86**(3):323-327. [doi:10.1016/j.fuel.2006.08.008]

Celik, M.B., 2008. Experimental determination of suitable ethanol-gasoline blend rate at high compression ratio for gasoline engine. *Applied Thermal Engineering*, **28**(5-6): 396-404. [doi:10.1016/j.applthermaleng.2007.10.028]

Charoenphonphanich, C., Ornman, P., Karin, P., Kosaka, H., Chollacoop, N., 2011. Experimental Investigation in Combustion Characteristics of Ethanol-Gasoline Blends for Stratified Charge Engine. SAE Technical Paper,

2011-32-0551. [doi:10.4271/2011-32-0551]

Cowart, J., Cheng, W., 1999. Intake Valve Thermal Behavior during Steady-State and Transient Engine Operation. SAE Technical Paper, 1999-01-3643. [doi:10.4271/1999-01-3643]

Hendricks, E., Vesterholm, T., Sorenson, S., 1992. Nonlinear, Closed Loop, SI Engine Control Observers. SAE Technical Paper, 920237. [doi:10.4271/920237]

Joshi, S., Lave, L., Maclean, H., Lankey, R., 2000. A Life Cycle Comparison of Alternative Transportation Fuels. SAE Technical Paper, 2000-01-1516. [doi:10.4271/2000-01-1516]

Kar, K., Last, T., Haywood, C., Raine, R., 2008. Measurement of Vapor Pressures and Enthalpies of Vaporization of Gasoline and Ethanol Blends and Their Effects on Mixture Preparation in an SI Engine. SAE Technical Paper, 2008-01-0317. [doi:10.4271/2008-01-0317]

Kiencke, U., Nielsen, L., 2005. Automotive Control Systems for Engine, Driveline, and Vehicle. Springer-Verlag Berlin Heidelberg, Germany, p.99-104.

Lauer, T., Heiss, M., Klein, M., 2011. Impact of the Wall Film Formation on the Full Load Performance of an Engine Operated with the Ethanol Blend E85. SAE Technical Paper, 2011-32-0535. [doi:10.4271/2011-32-0535]

Maloney, P., 1999. An Event-Based Transient Fuel Compensator with Physically Based Parameters. SAE Technical Paper, 1999-01-0553. [doi:10.4271/1999-01-0553]

Najafi, G., Ghobadian, B., Tavakoli, T., Buttsworth, D.R., Yusaf, T.F., Faizollahnejad, M., 2009. Performance and exhaust emissions of a gasoline engine with ethanol blended gasoline fuels using artificial neural network. *Applied Energy*, **86**(5):630-639. [doi:10.1016/j.apenergy.2008.09.017]

Pontoppidan, M., Damasceno, F., 2008. The Integral Flex-Vehicle Mixture Control of Alcohol-Based Bio-Fuels. SAE Technical Paper, 2008-01-0437. [doi:10.4271/2008-01-0437]

Shan, X., Burl, J., Jankovic, M., Cooper, S., 2008. Transient Fuel X-Tau Parameter Estimation Using Short Time Fourier Transform. SAE Technical Paper, 2008-01-1305. [doi:10.4271/2008-01-1305]

Yao, D., 2010. Research on Air-Fuel Ratio Control of SI Engines Burning Ethanol-Gasoline Blends. PhD Thesis, Zhejiang University, Hangzhou, China (in Chinese).